DOI 10.1007/s11003-019-00221-2

Materials Science, Vol. 54, No. 4, January, 2019 (Ukrainian Original Vol. 54, No. 4, July–August, 2018)

SPECIFIC FEATURES OF DEFORMATION OF THE NITINOL ALLOY AFTER ELECTROLYTIC HYDROGENATION

V. P. Iasnii,[1] H. M. Nykyforchyn,[2] O. T. Tsyrul'nyk,[2] and O. Z. Student[2,3]

UDC 539.3

Specific features of the effect of hydrogenation on the susceptibility of a Ni–Ti alloy with shape memory to deformation are determined with the use of metallographic, electrochemical, and mechanical studies. Three sections are detected in the tensile curves of the specimens of nickel–titanium alloy in the initial state. The first section is linear due to the elastic deformation of the alloy with initial austenitic structure. The second section is nonlinear and associated with pseudoelastic structural transformations of the original austenitic structure into a martensitic structure. The third section is also linear and caused by the elastic deformation of martensite formed in the course of deformation of austenite. After hydrogenation of the Ni–Ti alloy, the pseudoelastic structural transformation starts at a somewhat lower level of stresses than without hydrogenation. In this case, the specimens are destroyed after the termination of this transformation for a much lower level of plasticity than in the nonhydrogenated alloy. It is assumed that the electrolytic hydrogenation of the alloy promotes the formation of a very brittle hydride phase on the surface of Ti-type inclusions revealed in the structure of alloy in the initial state. Its thickness is determined by the duration of the process of hydrogenation rather than by the current used for hydrogenation.

Keywords: Ni–Ti alloy, electrolytic hydrogenation, tensile loading, deformation behavior.

The alloys with shape memory effect possess unique properties. Therefore, they are extensively used in the aerospace industry [1], biomedicine [2–4], nuclear power industry, civil and industrial engineering [5–9], etc. The most popular alloy with shape memory effect is Nitinol [10]. Despite the fact that materials of this kind belong to the class of functional materials, they must satisfy certain requirements imposed on the level of their structural strength in the course of structural-and-phase transformations running in these materials under the influence of temperature [11] or strains [12] and depending on the influence of ambient and working hydrogenating corrosive media [13]. It is well known from the literature that, under the influence of hydrogen, the level of plasticity decreases [14], the shape memory effect disappears [15], and the fatigue life of Ni–Ti alloys decreases [16]. Moreover, the plasticity and strength of Ni–Ti alloys decrease starting from hydrogen concentrations of about 10–50 ppm^{-1} [17–19]. In view of these facts, it is necessary to study the influence of hydrogen on the functional properties of the alloy with shape memory on the one hand and on its mechanical behavior on the other hand.

The aim of the present work is to study the influence of hydrogen absorbed by the nickel-titanium alloy with shape memory on the specific features of deformation of this alloy.

[1] Pulyui Ternopil' National Technical University, Ukraine.

[2] Karpenko Physicomechanical Institute, Ukrainian National Academy of Sciences, Lviv, Ukraine.

[3] Corresponding author; e-mail: student@ipm.lviv.ua.

Translated from Fizyko-Khimichna Mekhanika Materialiv, Vol. 54, No. 4, pp. 124–130, July–August, 2018. Original article submitted June 12, 2018.

 1068-820X/19/5404–0582

Fig. 1. General view of a specimen weakened by a notch.

Methodical Aspects of the Tests

We study rods made of the Nitinol alloy ($Ni_{55.8}Ti_{44.2}$). The delivery certificate specifies the following chemical composition of the alloy (wt.%): 55.78 Ni, 0.005 Co, 0.005 Cu, 0.005 Cr, 0.012 Fe, 0.005 Nb, 0.032 C, 0.001 H, 0.040 O, 0.001 N, and balance Ti. Its mechanical characteristics are as follows: the ultimate strength is equal to 855 MPa, the yield limit to 228 MPa, and the relative elongation to 19%.

Cylindrical specimens with a 5-mm net section of the working part were tested by tension in a UME-10T installation (Fig. 1). Some specimens were electrolytically hydrogenated prior to the mechanical tests. As a working medium, we used an aqueous solution of hydrofluoric acid with pH 2. After hydrogenation, the specimens were loaded in air for a velocity of motion of an active clamp equal to 1 mm/h.

The metallographic studies of the alloy were carried out on a EVO-40XVP scanning electron microscope equipped with the INCA Energy-350 system for the X-ray diffraction spectral microanalysis.

Experimental Results and Discussion

Metallographic Studies. Independently of the cross section (longitudinal or transverse) in which the structure was analyzed, the grains mainly have a polygonal morphology in the form of almost equiaxial grains (Fig. 2).

Hence, the shape of the grains does not allow us to speak about the presence of texture in the initial state of the alloy. Therefore, we assume that, in the final stage of production of rods made of Nitinol, they are subjected to high-temperature thermal treatment guaranteeing the complete recrystallization of the alloy. The structure of the alloy morphologically corresponds to austenite with almost parallel twins within the limits of separate grains. These twins cross the grains in the form of packages. However, the twins were extended from one boundary of a grain to the other its boundary not in all cases. We observed a clear relationship between the orientation of twins and the crystallography of grains because the orientation of twin packages varied from grain to grain.

In the structure of the alloy, against the background of austenitic matrix, we observe the presence of quite large inclusions (up to 10 μm in size). The inclusions have round cross-sectional shapes and are almost identical in the longitudinal and transverse microsections. The nature of inclusions in the Nitinol structure was clarified with the help of X-ray diffraction spectral microanalysis. It was discovered that the main element in the composition of these inclusions is titanium (~ 98 wt.% on the average), whereas the composition of the matrix includes 44 wt.% of titanium and 56 wt.% of nickel, which approximately corresponds to the composition of the alloy specified in the delivery certificate.

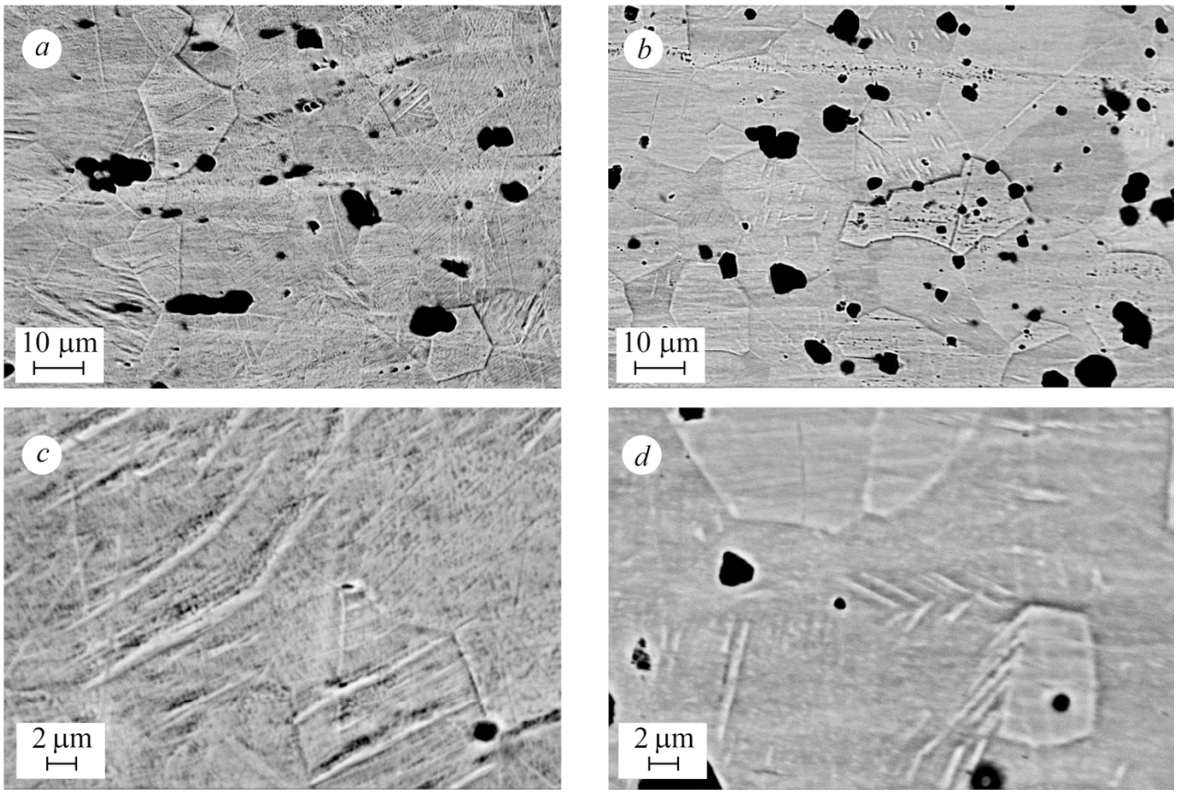

Fig. 2. Structures of the Nitinol alloy on polished surfaces in the longitudinal (a, c) and transverse microsections (b, d) of a rolled rod.

Mechanical Studies. The specimens were cyclically loaded by tension with stepwise increase in the maximum level of stresses in each subsequent loading cycle. In the first loading cycle, after the initial linear section characterized by the elastic deformation of the alloy, we revealed a nonlinear section caused by the decrease in stresses. Therefore, the next loading cycles were carried out in the following way: three additional cycles were realized until the section characterized by a decrease in stresses disappeared (Fig. 3a). Then the specimen was held in the unloaded state for 24 h and three more loading cycles were performed (Fig. 3b). After this, the specimen was loaded by tension with a velocity of motion of an active clamp equal to 1 mm/h to fracture.

The obtained diagrams enable us to conclude that, in general, it is possible to distinguish three sections in the curves of tensile loading of the specimens (Fig. 3): linear sections whose slopes correspond to the slope of the curve *A* in Fig. 3b; nonlinear sections in the stage of lowering of the level of stresses, and linear sections whose slopes correspond to the straight line *B* in Fig. 3b.

It is clear that the first linear section characterizes the elastic deformation of initial austenite up to the start of its pseudoelastic structural transformation into martensite (Fig. 3a). It starts under stresses higher than 505 MPa. As already indicated, a nonlinear section with characteristic decrease in stresses appears in the first loading cycle after the linear section. It was assumed that the structural transformation of the original austenite into martensite occurs first as the level of stresses increases. On attainment of a certain maximum value, this transformation is accompanied by the relaxation of stresses and is practically completed on the same level of stresses as in the initial state. In the second loading cycle, the character of the diagram for the investigated alloy is similar but the decrease in stresses is manifested not so clearly. In the third cycle, we observe a plateau-like section in the diagram of transformation of the initial austenite into martensite corresponding to somewhat higher stresses.

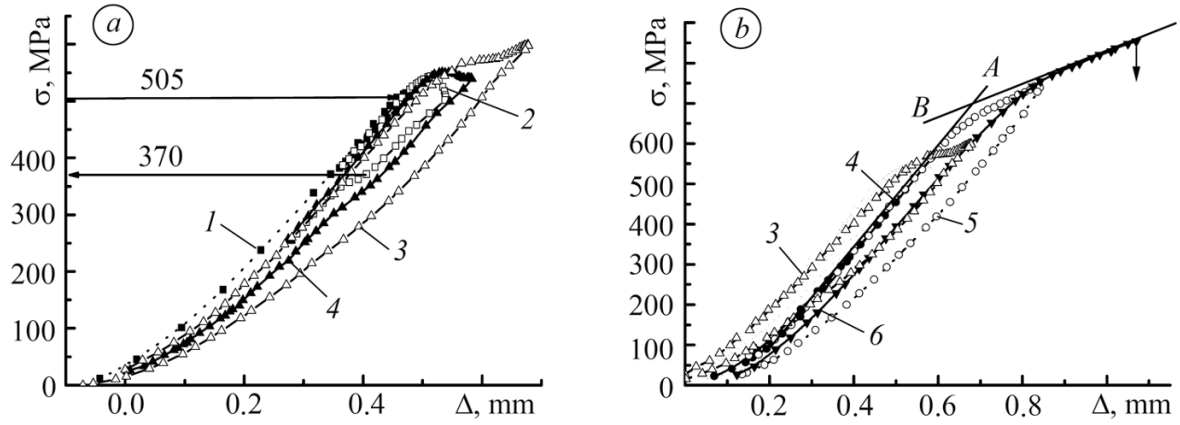

Fig. 3. Loading-unloading cycles for a specimen made of the Nitinol alloy in the intact state prior to (a) and after (b) the completion of the martensitic transformation caused by deformation. The extrapolation lines for two parts of the loading diagram of the specimen (A and B) after the completed martensitic transformation caused by deformation: (1–6) numbers of cycles.

In the curves of unloading, after the first rectilinear sections, we see nonlinear sections obviously caused by the reverse pseudoelastic structural transformation of martensite into austenite. In view of the fact that the clearly expressed transformation is observed only in the first cycle, we can also assume that the transformation of initial austenite into martensite occurs in two stages.

In the first loading cycle, martensite is formed in the section corresponding to a decrease in stresses. Its structure is transformed into the austenitic structure in course of unloading down to ~ 370 MPa. In the second cycle, the decrease in stresses is less pronounced. Hence, the indicated transformation of martensite into austenite is not so clear, most likely due to the formation of martensite with different structure whose transformation into austenite is complicated. As the level of strains in a loading cycle increases, the transformation of martensite into austenite in the course of unloading becomes complicated and terminates at lower stresses.

In the third loading cycle, we observe an increase in the austenite–martensite transformation resistance. The procedure of holding of the specimen for one day after the first three loading cycles exerts no influence on the mechanical behavior of the alloy. In the fourth cycle, in the course of loading up to stresses higher than at the origin of the austenite–martensite transformation in the first three cycles, the curve of unloading practically coincides with the loading curve (Fig. 3b). As the maximum load increases in the fifth and sixth cycles, the austenite–martensite transformation resistance continues to increase. Under stresses of about 850 MPa, the specimen is destroyed.

The absolute elongation of the specimen $\Delta = 0.255$ mm. It is estimated according to the tensile loading curve. It is difficult to estimate the relative narrowing of the alloy because, after fracture, the martensite–austenite transformation with possible changes in the shape of the specimen had already happened and, therefore, the actual diameter of the specimen at the time of fracture remains unclear. The indicated low plasticity of the alloy serves as an indication of its high brittleness. Almost immediately after the initiation of a microcrack, we observe its spontaneous (supercritical) propagation without formation of visible signs of shear in the zone of final fracture (Fig. 4).

To estimate the influence of hydrogen on mechanical characteristics of the alloy, we used two modes of hydrogenation of specimens: (I) at a current density of 0.1 mA/cm^2 for 65 h and (II) at a current density of 0.01 mA/cm^2 for 290 h.

The specimen hydrogenated in mode I was destroyed in the first loading cycle (practically immediately after the completion of the austenite–martensite transformation) in the transition to the section of elastic deformation

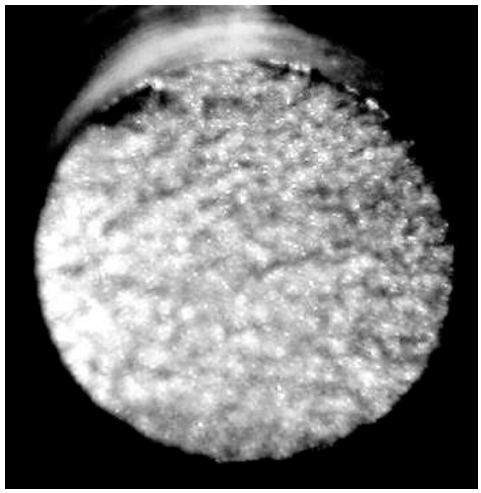

Fig. 4. General view of the fracture surface of a specimen made of the Nitinol alloy in the initial state.

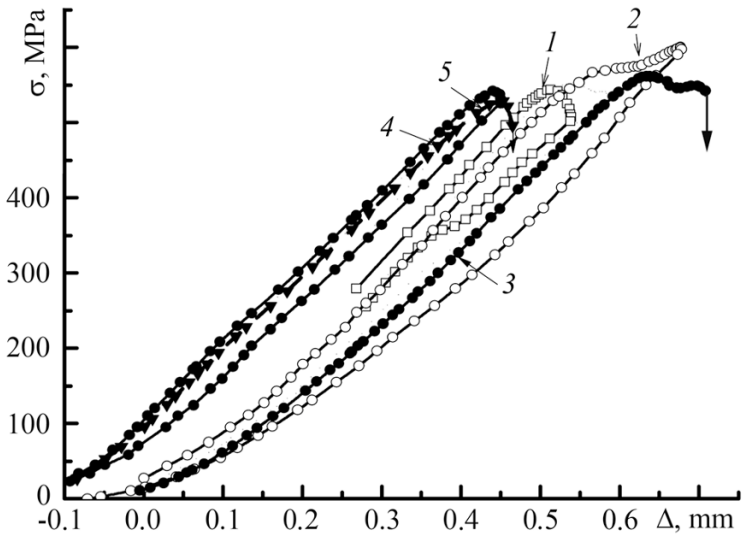

Fig. 5. Effect of hydrogenation on the curves of tensile cyclic loading of specimens made of the Nitinol alloy: (1, 2) first and second loading cycles for the alloy in the initial state (without hydrogenation); (3) first cycle of loading after hydrogenation in mode I; (4, 5) first and second cycles of loading of the alloy after hydrogenation in mode II.

of martensite under stresses of ~ 550 MPa (Fig. 5). This reveals a very low crack-initiation resistance of hydrogenated martensite, i.e., a high susceptibility of the alloy to hydrogen embrittlement. This is also confirmed by its very low plasticity ($\Delta = 0.109$ mm).

In the case of testing of the specimens hydrogenated in mode II, the austenite-martensite transformation starts at somewhat lower stresses of about 520 MPa. The hydrogenated specimen was destroyed in the second loading cycle, possibly immediately after the completion of the transformation of austenite into martensite under a stress of about 520 MPa (because the same transformation in the nonhydrogenated alloy terminated just at the indicated level of stresses). For three types of specimens, the pseudoelastic strains are practically identical in the sections, where the stresses decrease (Fig. 5). The plasticity of the specimens hydrogenated in mode II is lower than for mode I ($\Delta = 0.086$ mm). Hence, the specimens hydrogenated in mode II fail at lower levels of stresses and exhibit, in this case, lower values of plasticity.

This result seems to be somewhat unexpected because the current observed in the process of hydrogenation in mode II is lower than in the case of mode I by an order of magnitude. It could be expected that the dependences of fracture stresses and plasticity on the hydrogenation current (opposite to the traditional dependences) are caused by the formation of a very brittle hydride phase on the surface of alloy in the course of electrolytic hydrogenation of the specimen rather than by the hydrogen embrittlement of the martensitic phase, which is sensitive to the content of absorbed hydrogen. Indeed, titanium alloys used for the production of hydrogen storage batteries are characterized by the formation of a hydride phase with the corresponding stoichiometric composition for certain concentrations of hydrogen [20]. Note that the hydrogen concentration in the surface layer of hydride is determined not by the hydrogenation current but by the stoichiometric composition of the formed hydride. Therefore, the intensity of diffusion and, hence, the thickness of the hydride layer are obviously determined by the duration of hydrogenation. In the second mode of hydrogenation, it is almost five times larger, which explains the observed effect.

In addition, it is necessary to take into account the fact that the inclusions detected in the structure of the alloy correspond (in the content of elements) to almost pure titanium. Hence, these inclusions can absorb hydrogen especially intensely and, therefore, serve as the sites of formation of brittle titanium hydrides. In view of their sizes (up to 10 μm) and a fairly uniform density of their arrangement, it is possible to assume that not only the level of brittleness of these hydrides is responsible for the decrease in the brittle-fracture resistance of the hydrogenated alloy but also the influence of hydrides as relatively sharp stress concentrators in the martensitic matrix can also play a significant role in this process.

The obtained results reveal the necessity of a more detailed investigation of the influence of hydrogen on the mechanical behavior of Nitinol due to the kinetic restrictions imposed on its penetration from corrosive medium depending on the protective properties of the surface films, compositions of the working and technological media, hydrogen content, and hence, the thickness of the hydride phase on the surface of titanium inclusions in the austenitic matrix of the alloy. It is also important to study the kinetics of hydrogenation of the alloy in the course of pseudoelastic transformation because it is known that the self-diffusion and diffusion of alloying interstitial and substitutional elements becomes much more intense in the presence of these transformations of the crystal lattice [21].

CONCLUSIONS

In the tensile loading curves of the nickel-titanium alloy in the initial state, we observe three sections: a linear section of elastic deformation of initial austenite, a nonlinear section corresponding to the pseudoelastic structural transformation of the initial austenite into martensite, and a linear section of elastic deformation of martensite. The pseudoelastic structural transformation of initial austenite into martensite occurs as the level of stresses increases; as a certain maximum level of stresses is attained, this transformation is accompanied by a relaxation of stress and terminates almost on the same level as at the onset of transformation. In the initial state, the Nitinol specimens are destroyed in a brittle way almost immediately after the completion of elastic deformation of the martensitic structure without noticeable signs of the formation of "elongation lips." Under the conditions of hydrogenation of Nitinol, the pseudoelastic structural transformation originates at a somewhat lower level of stresses than without hydrogenation. In this case, the specimens fail after the completion of the transformation and exhibit much lower plasticity as compared with the nonhydrogenated alloy. It is assumed that, in the process of electrolytic hydrogenation, we observe the formation of conditions required for the appearance of a very brittle hydride phase on the Nitinol surface. Moreover, the thickness of this phase is determined not by the hydrogenation current but by the duration of the process.

The present work was financially supported by the State Foundation for Fundamental Research within the framework of the Competitive Project 0117U003885.

REFERENCES

1. P. Iasnii and V. Iasnii, *Damping Unit for the Transportation of Large-Size Structures* [in Ukrainian], Patent 116582 Ukraine MPK F16F 7/12, Publ. on 25.05.2017; Bull. No. 10.
2. Y. Oshida, R. Sachdeva, Sh. Miyazaki, and S. Fukuyo, "Biological and chemical evaluation of Ti-Ni alloys," *Martens. Transform. Trans. Tech. Publ.,* **56**, 705–710 (1991).
3. Z. Lekston, J. Drugacz, and H. Morawiec, "Application of superelastic NiTi wires for mandibular distraction," *Mater. Sci. Eng. A,* **378**, Nos. 1–2, 537–541 (2004).
4. G. Rondelli, "Corrosion resistance tests on NiTi shape memory alloy," *Biomaterials,* **17**, 2003–2008 (1996).
5. H. Ma, T. Wilkinson, and C. Cho, "Feasibility study on a self-centering beam-to-column connection by using the superelastic behavior of SMAs," *Smart Mater. Struct.,* **16**, No. 5, 1555–1563 (2007).
6. A. Isalgue, F. C. Lovey, P. Terriault, F. Martorell, R. M. Torra, and V. Torra, "SMA for dampers in civil engineering," *Mater. Trans.,* **47**, No. 3, 682–690 (2006).
7. H. Ma and M. C. H. Yam, "Modeling of a self-centering damper and its application in structural control," *J. Constr. Steel Res.,* **67**, No. 4, 656–666 (2011).
8. V. Torra, C. Auyuet, G. Carreras, L. Dieng, F. C. Lovey, and P. Terriault, "The SMA: An effective damper in civil engineering that smoothes oscillations," *Mater. Sci. Forum,* **706–709**, 2020–2025 (2012).
9. P. Yasniy, M. Kolisnyk, O. Kononchuk, and V. Iasnii, "Calculation of constructive parameters of SMA damper," *Sci. J. TNTU,* **88**, No. 4, 7–15 (2017).
10. G. Kauffman and I. Mayo, "The story of Nitinol: the serendipitous discovery of the memory metal and its applications," *Chem. Educ.,* **2**, No. 2, 1–21 (1997).
11. V. P. Iasnii and R. Junga, "Phase transformations and mechanical properties of the Nitinol alloy with shape memory," *Fiz.-Khim. Mekh. Mater.,* **54**, No. 3, 107–111 (2018).
12. D. J. Hartl and D. C. Lagoudas, "Aerospace applications of shape memory alloys," *Proc. of the Inst. Mech. Eng.: J. Aerospace Eng.,* **221**, Part G, 535–582 (2007).
13. A. L. Quintanilla, *Shape Memory Alloys,* Dissertation, Delft Univ. of Technology (2016).
14. F. Gamaoun, I. Skhiri, T. Bouraoui, and T. Ben Zineb, "Hydrogen effect on the austenite–martensite transformation of the cycled Ni–Ti alloy," *J. Intellig. Mater. Syst. Struct.,* **25**, No. 8, 980–988 (2014).
15. I. Kireeva, Yu. Platonova, and Yu. Chumlyakov, "Effect of hydrogen on the two-way shape memory effect in TiNi single crystals," *Mater. Today,* **4**, No. 3, Part B, 4773–4777 (2017).
16. J. Sheriff, A. R. Pelton, and R. A. Pruitt, "Hydrogen effects on Nitinol fatigue," in: *Proc. Internat. Conf. on Shape Memory and Superelastic Technologies,* SMST-2004, M. Mertman (editor), ASM International, Baden-Baden (2004), pp. 111–119.
17. K. Yokoyama, T. Ogawa, K. Asaoka, J. Sakai, and M. Nagumo, "Degradation of tensile strength of Ni–Ti superelastic alloy due to hydrogen absorption in methanol solution containing hydrochloric acid," *Mater. Sci. Eng.: A,* **360**, Nos. 1–2, 153–159 (2003).
18. K. Kaneko, K. Yokoyama, K. Moriyama, K. Asaoka, and J. Sakai, "Degradation in the performance of orthodontic wires caused by hydrogen absorption during short-term immersion in 2.0% acidulated phosphate fluoride solution," *Angle Orthodontist,* **74**, No. 4, 487–495 (2004).
19. K. Yokoyama, K. Kaneko, K. Moriyama, K. Asaoka, J. Sakai, and M. Nagumo, "Hydrogen embrittlement of Ni-Ti superelastic alloy in fluoride solution," *J. Biomed. Mater. Res.,* **65A**, 182–187 (2003).
20. V. N. Kudiyarov, A. M. Lider, N. S. Pushilina, and N. A. Timchenko, "Specific features of the accumulation and distribution of hydrogen in the course of saturation of VT1-0 titanium alloy by the electrolytic method and from a gas atmosphere," *Zh. Tekh. Fiz.,* **84**, Issue 9, 117–121 (2014).
21. V. I. Pokhmurs'kyi and V. V. Fedorov, *Influence of Hydrogen on the Diffusion in Metals* [in Ukrainian], Enei, Lviv (1998).